Transp Porous Med
DOI 10.1007/s11242-009-9379-0

Turbulent Flow Around Fluid–Porous Interfaces Computed with a Diffusion-Jump Model for k and ε Transport Equations

Marcelo J. S. De Lemos

Received: 4 March 2008 / Accepted: 5 March 2009

Abstract Flow over vegetation and bottom of rivers can be characterized by some sort of porous structure of irregular surface through which a fluid permeates. Also, in engineering systems, one can have components that make use of a working fluid flowing over irregular layers of porous material. This article presents numerical solutions for such hybrid medium, considering here a channel partially filled with a flat porous layer saturated by a fluid flowing in turbulent regime. One unique set of transport equations is applied to both the regions. A diffusion-jump model for both the turbulent kinetic energy and its dissipation rate, across the interface, is presented and discussed upon. The discretization steps taken for numerically accommodating such model in the system of algebraic equations are presented. Numerical results show the effects of Reynolds number, porosity, and permeability on mean and turbulence fields. Results indicate that when negative values for the stress jump coefficient are applied, the peak of the turbulent kinetic energy distribution occurs at the macroscopic interface.

Keywords Turbulence modeling · Porous media · Volume-average · Time-average · Interface · Stress jump · Two-equation model

List of Symbols

c_F	Forchheimer coefficient
c_1, c_2, c_k, c_μ	Constant in turbulence model
$\mathbf{D}$	Deformation rate tensor, $\mathbf{D} = [\nabla \mathbf{u} + (\nabla \mathbf{u})^{\mathrm{T}}]/2$
G^{i}	Production rate of k due to the porous matrix, $G^{\mathrm{i}} = c_k \rho \phi \langle k \rangle^{\mathrm{i}} \lvert \bar{\mathbf{u}}_{\mathrm{D}} \rvert / \sqrt{K}$
H	Distance between the channel walls

M. J. S. De Lemos (✉)
Departamento de Energia - IEME, Instituto Tecnológico de Aeronáutica - ITA,
12228-900 São José dos Campos, SP, Brazil
e-mail: delemos@ita.br

Published online: 04 April 2009

$\mathbf{I}$	Unit tensor
k	Turbulent kinetic energy per unit mass, $k = \overline{\mathbf{u}' \cdot \mathbf{u}'}/2$
$\langle k \rangle^{\mathrm{v}}$	Volume (fluid + solid) average of k
$\langle k \rangle^{\mathrm{i}}$	Intrinsic (fluid) average of k
K	Permeability
L	Axial length of periodic section of channel
p	Thermodynamic pressure
$\langle p \rangle^{\mathrm{i}}$	Intrinsic (fluid) average of pressure p
P^{i}	Production rate of k due to mean gradients of $\bar{\mathbf{u}}_{\mathrm{D}}$, $P^{\mathrm{i}} = -\rho \langle \overline{\mathbf{u}'\mathbf{u}'} \rangle^{\mathrm{i}} : \nabla \bar{\mathbf{u}}_{\mathrm{D}}$
$\overline{\mathbf{R}}$	Time average of total drag per unit volume
Re_{H}	Reynolds number based on the channel height, $Re_{\mathrm{H}} = \rho \, \lvert \bar{\mathbf{u}}_{\mathrm{D}} \rvert \, H/\mu$
s	Clearance for unobstructed flow
S_{φ}	Source term
$\bar{\mathbf{u}}$	Microscopic time-averaged velocity vector
$\langle \bar{\mathbf{u}} \rangle^{\mathrm{i}}$	Intrinsic (fluid) average of $\bar{\mathbf{u}}$
$\bar{\mathbf{u}}_{\mathrm{D}}$	Darcy velocity vector, $\bar{\mathbf{u}}_{\mathrm{D}} = \phi \, \langle \bar{\mathbf{u}} \rangle^{\mathrm{i}}$
$\bar{\mathbf{u}}_{\mathrm{Di}}$	Darcy velocity vector at the interface
$\bar{\mathbf{u}}_{\mathrm{Dp}}$	Darcy velocity vector parallel to the interface
$u_{\mathrm{Dn}}, u_{\mathrm{Dp}}$	Components of Darcy velocity at interface along η (normal) and ξ (parallel) directions, respectively.
$u_{\mathrm{D_i}}, v_{\mathrm{D_i}}$	Components of Darcy velocity at interface along x and y, respectively
x, y	Cartesian coordinates

Greek Symbols

$\beta, \beta_{\mathrm{t}}$	Interface stress jump coefficient for mean and turbulent flow fields, respectively
μ	Fluid dynamic viscosity
μ_{eff}	Effective viscosity for a porous medium
$\mu_{\mathrm{t}\phi}$	Macroscopic turbulent viscosity
ε	Dissipation rate of k, $\varepsilon = \mu \overline{\nabla \mathbf{u}' : (\nabla \mathbf{u}')^{\mathrm{T}}}/\rho$
$\langle \varepsilon \rangle^{\mathrm{i}}$	Intrinsic (fluid) average of ε
ρ	Density
ϕ	Porosity
φ	General dependent variable
η, ξ	Generalized coordinates
$\sigma_k, \sigma_\varepsilon$	Turbulent Prandtl numbers for k and ε, respectively.

1 Introduction

Investigation of flow over layers of permeable media has many applications in several environmental and engineering analyses. Turbulent atmospheric boundary layer over forests under fire (Zhou and Pereira 2000), canopy flow (Raupach and Shaw 1982, Finnigan 2000) flow over vegetation (Poggi and Katul 2007) and crop fields (Hoffmann 2004), currents at the bottom of rivers (Lane and Hardy 2002) and water channels (White and Nepf 2003, Nepf and Ghisalberti 2008), as well as grain storage and drying, are examples of flows which can be characterized by some sort of porous layer over which a fluid permeates. Also, practical analysis of engineering flows can further benefit from more realistic mathematical and numerical modeling, as in the case of shell-and-tube heat exchangers (Prithiviraj and Andrews 1998) and nuclear reactor core (Sha 1981), for example, where the rod bundles can be seen, in a macroscopic view, as a permeable medium.

When the domain of analysis presents a macroscopic interfacial area between a porous substrate and a clear flow region, the literature proposes the existence of a discontinuity in the momentum diffusion flux between the two media (Ochoa-Tapia and Whitaker 1995a,b). Analytical solutions involving such models have been published (Kuznetsov 1996, 1997, 1999). Also, in such works, volume average properties for a homogenous treatment of flow in porous media were obtained by means of the Volume-Average Theorem, VAT (Whitaker 1969, Gray and Lee 1977).

Purely numerical solutions for two-dimensional hybrid medium (porous region–clear flow) in an isothermal channel have been considered in de Lemos and Pedras (2000) based on the turbulence model proposed in Pedras and de Lemos (2000, 2001a,b,c, 2003). That work has been developed under the double decomposition concept, which has been reviewed in an article (de Lemos 2005a) and thoroughly detailed in a book (de Lemos 2006), as well as extended to non-buoyant heat transfer (Rocamora and de Lemos 2000a), buoyant flows (de Lemos and Braga 2003, Braga and de Lemos 2004), mass transfer (de Lemos and Mesquita 2003), double diffusion (de Lemos and Tofaneli 2004) and moving porous beds (de Lemos 2008). Non-isothermal flows in channels past a porous obstacle (Rocamora and de Lemos 2000b) and through a porous insert have also been presented (Assato et al. 2005). In all previous works of Rocamora and de Lemos (2000b) and Assato et al. (2005), the interface boundary condition considered a continuous function for the stress field across the interface.

Recently, the interface jump condition has been investigated for laminar flows, either considering non-linear effects in momentum equation as well as neglecting the Forchheimer term in the macroscopic model (Silva and de Lemos 2003a). Therein, the authors simulated laminar flow over such interfaces and validated their results against analytical solutions by Kuznetsov (1996, 1997, 1999). Such work was based on the numerical methodology proposed for hybrid media and applied by de Lemos and Pedras (2000), Rocamora and de Lemos (2000b), and Assato et al. (2005). The same numerical technique has been applied for computing turbulent flow (Silva and de Lemos 2003b) in a channel partially filled with a flat layer of porous material. Flows over wavy interfaces were also computed for both laminar (Silva and de Lemos 2003c) and turbulent flows (de Lemos and Silva 2003). There, the authors made use of the shear stress jump condition at the interface. A distinct line of investigation on turbulent flow over permeable media is based on the assumption that within the porous layer, the flow remains laminar (Kuznetsov 2004), which, in turn, precludes application of such methodology to flows through highly permeable media as atmospheric boundary layer over forests or crop fields.

Further, fine flow computations and experiments of flow over and inside a bed of rods in a two-dimensional channel have been presented (Prinos et al. 2003). Three-dimensional computational studies simulating flow over a layer formed by cubic blocks (Breugem and Boersma 2005) also emphasize that depending on the permeable structure shape, turbulence may exists inside the porous bed and, as such, a turbulence model must be employed.

As seen, all models above considered either a flat or a rough (wavy) macroscopic interface limiting the porous substrate. The stress jump condition for the momentum equations was applied, but in most publications so far, no such flux discontinuity for the $\langle k\rangle^{v}$-equation has been considered. Motivated by that, de Lemos (2005b) proposed a model that assumes diffusion fluxes of turbulent kinetic energy and its dissipation rate on both sides of the interface to be unequal, which differed from all studies presented up to then. In de Lemos (2005b), however, no specific detail was given on the treatment of the $\langle\varepsilon\rangle^{\mathrm{i}}$-equation. Therein, only for the $\langle k\rangle^{\mathrm{v}}$-equation, the diffusion jump concept was commented upon.

The purpose of this contribution is therefore twofold. First, to present the proposed model for the diffusion-jump for the $\langle\varepsilon\rangle^{\mathrm{i}}$-equation, which was used but not presented in full in de Lemos (2005b). Second, to explore and further document such proposals, investigating the behavior of $\langle k\rangle^{\mathrm{v}}$ across the interface as medium properties, such as permeability and porosity, are varied.

2 Macroscopic Mathematical Model

2.1 Geometry and Governing Equations

The flow under consideration is schematically shown in Fig. 1a, where a channel is partially filled with a layer of a porous material. A constant property fluid flows longitudinally from left to right permeating through both the clear region and the porous structure. The case in Fig. 1a uses symmetry boundary condition at the channel center ($y = 0$). Also, H is the distance in between the channel walls and s is the clearance for the non-obstructed flow passage. It should be emphasized that the class of flow under consideration involves porous substrates having high porosity and high permeability.

A macroscopic form of the governing equations is obtained by taking the volumetric average of the entire equation set. In this development, the porous medium is considered to be rigid and saturated by the incompressible fluid.

The macroscopic continuity equation is given by

$$\nabla \cdot \overline{\mathbf{u}}_{\mathrm{D}} = 0, \tag{1}$$

where the Dupuit–Forchheimer relationship, $\overline{\mathbf{u}}_{\mathrm{D}} = \phi\, \langle\overline{\mathbf{u}}\rangle^{\mathrm{i}}$, has been used and $\langle\overline{\mathbf{u}}\rangle^{\mathrm{i}}$ identifies the intrinsic (liquid) average of the local velocity vector $\overline{\mathbf{u}}$ (Gray and Lee 1977). Equation 1 represents the macroscopic continuity equation for an incompressible fluid in a rigid porous medium.

The macroscopic time-mean Navier–Stokes (NS) equation for an incompressible fluid with constant properties can be written as,

$$\rho\left[\frac{\partial}{\partial t}\left(\phi\langle\overline{\mathbf{u}}\rangle^{\mathrm{i}}\right) + \nabla\cdot\left(\phi\langle\overline{\mathbf{u}}\,\overline{\mathbf{u}}\rangle^{\mathrm{i}}\right)\right]$$
$$= -\nabla\left(\phi\langle\overline{p}\rangle^{\mathrm{i}}\right) + \mu\nabla^{2}\left(\phi\langle\overline{\mathbf{u}}\rangle^{\mathrm{i}}\right) + \nabla\cdot\left(-\rho\phi\langle\overline{\mathbf{u}'\mathbf{u}'}\rangle^{\mathrm{i}}\right) + \overline{\mathbf{R}}. \tag{2}$$

As usually done when treating turbulence with statistical tools, the correlation $-\rho\overline{\mathbf{u}'\mathbf{u}'}$ appears after application of the time-average operator to the local instantaneous NS equation. Applying further the volume-average procedure to the entire momentum equation (see Pedras and de Lemos 2001a for details), results in the term $-\rho\phi\langle\overline{\mathbf{u}'\mathbf{u}'}\rangle^{\mathrm{i}}$ of (2). This term is here recalled as the *Macroscopic Reynolds Stress Tensor* (MRST). In addition, $\overline{\mathbf{R}}$ in (2) represents the time-mean total drag per unit volume acting on the fluid by the action of the porous structure. A common model for it is known as the Darcy–Forchheimer extended model and is given by

$$\overline{\mathbf{R}} = -\left[\frac{\mu\phi}{K}\overline{\mathbf{u}}_{\mathrm{D}} + \frac{c_{\mathrm{F}}\phi\rho\,|\overline{\mathbf{u}}_{\mathrm{D}}|\overline{\mathbf{u}}_{\mathrm{D}}}{\sqrt{K}}\right], \tag{3}$$

where the constant c_{F} is known in the literature as the non-linear Forchheimer coefficient.

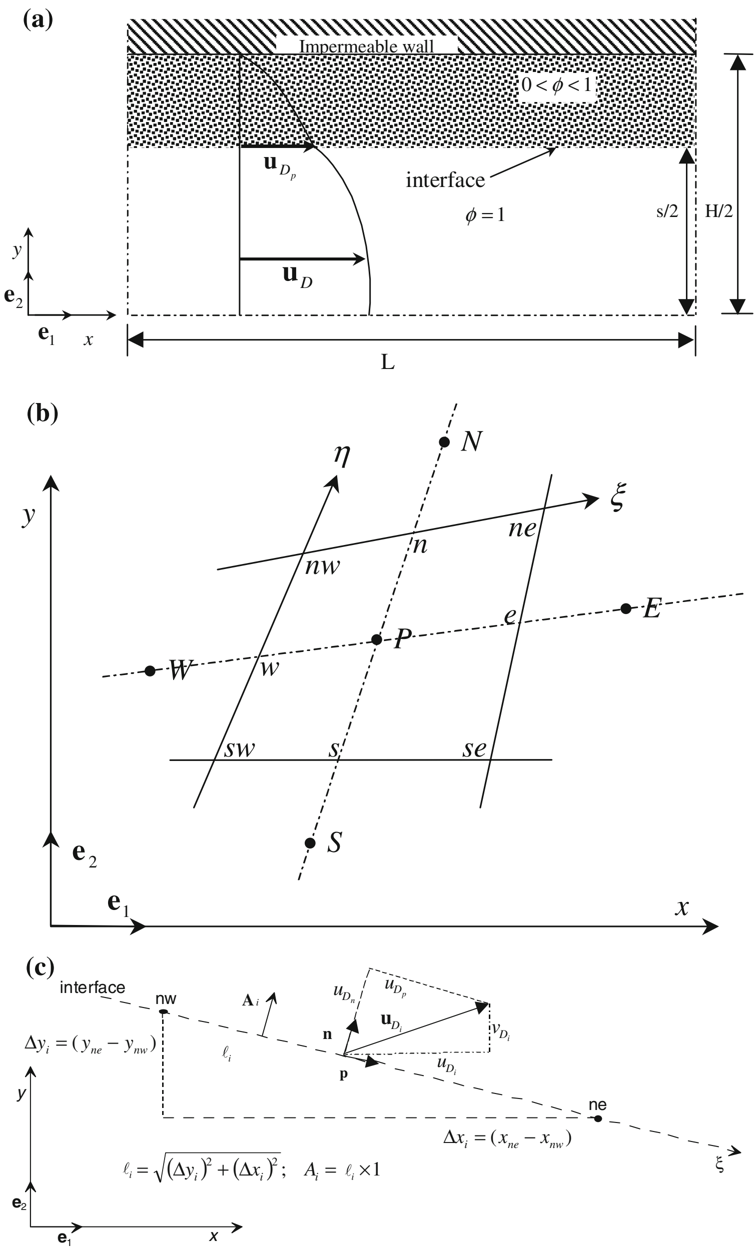

Fig. 1 Turbulent channel flow with porous material **a**, notation for control volume discretization **b**, and notation for interface treatment **c**

Then, making use again of the expression $\overline{\mathbf{u}}_D = \phi\, \langle \overline{\mathbf{u}} \rangle^i$ and (3), Eq. 2 can be rewritten as

$$\rho \left[\frac{\partial \overline{\mathbf{u}}_D}{\partial t} + \nabla \cdot \left(\frac{\overline{\mathbf{u}}_D\, \overline{\mathbf{u}}_D}{\phi} \right) \right]$$
$$= -\nabla \left(\phi \langle \overline{p} \rangle^i \right) + \mu \nabla^2 \overline{\mathbf{u}}_D + \nabla \cdot \left(-\rho \phi \langle \overline{\mathbf{u}' \mathbf{u}'} \rangle^i \right) - \left[\frac{\mu \phi}{K} \overline{\mathbf{u}}_D + \frac{c_F \phi \rho\, |\overline{\mathbf{u}}_D| \overline{\mathbf{u}}_D}{\sqrt{K}} \right]. \quad (4)$$

Further, a model for the MRST in analogy with the Boussinesq concept for clear fluid can be written as

$$-\rho\phi\langle\overline{\mathbf{u}'\mathbf{u}'}\rangle^{\mathrm{i}} = \mu_{\mathrm{t}\phi}2\langle\overline{\mathbf{D}}\rangle^{\mathrm{v}} - \frac{2}{3}\phi\rho\langle k\rangle^{\mathrm{i}}\mathbf{I}, \tag{5}$$

where

$$\langle\overline{\mathbf{D}}\rangle^{\mathrm{v}} = \frac{1}{2}\left[\nabla\left(\phi\langle\overline{\mathbf{u}}\rangle^{\mathrm{i}}\right) + \left[\nabla\left(\phi\langle\overline{\mathbf{u}}\rangle^{\mathrm{i}}\right)\right]^{\mathrm{T}}\right] \tag{6}$$

is the macroscopic deformation tensor, $\langle k\rangle^{\mathrm{i}}$ is the intrinsic average for k and $\mu_{\mathrm{t}\phi}$ is the macroscopic turbulent viscosity. The macroscopic turbulent viscosity, $\mu_{\mathrm{t}\phi}$, used in (5) is modeled similarly to the case of clear fluid flow, and a proposal for it was presented in Pedras and de Lemos (2001a) as

$$\mu_{\mathrm{t}\phi} = \rho c_{\mu}\langle k\rangle^{\mathrm{i}^2}/\langle\varepsilon\rangle^{\mathrm{i}}. \tag{7}$$

2.2 Macroscopic Equations for $\langle k\rangle^{\mathrm{i}}$and $\langle\varepsilon\rangle^{\mathrm{i}}$

Transport equations for $\langle k\rangle^{\mathrm{i}} = \langle\overline{\mathbf{u}'\cdot\mathbf{u}'}\rangle^{\mathrm{i}}/2$ and $\langle\varepsilon\rangle^{\mathrm{i}} = \mu\langle\overline{\nabla\mathbf{u}' : (\nabla\mathbf{u}')^T}\rangle^{\mathrm{i}}/\rho$ in their so-called High Reynolds Number form are proposed in Pedras and de Lemos (2001a) as

$$\rho\left[\frac{\partial}{\partial t}\left(\phi\langle k\rangle^{\mathrm{i}}\right) + \nabla\cdot\left(\overline{\mathbf{u}}_{\mathrm{D}}\langle k\rangle^{\mathrm{i}}\right)\right] = \nabla\cdot\left[\left(\mu + \frac{\mu_{\mathrm{t}\phi}}{\sigma_k}\right)\nabla\left(\phi\langle k\rangle^{\mathrm{i}}\right)\right] + P^{\mathrm{i}} + G^{\mathrm{i}} - \rho\phi\langle\varepsilon\rangle^{\mathrm{i}}, \tag{8}$$

where $P^{\mathrm{i}} = -\rho\langle\overline{\mathbf{u}'\mathbf{u}'}\rangle^{\mathrm{i}} : \nabla\overline{\mathbf{u}}_{\mathrm{D}}$, $G^{\mathrm{i}} = c_k\rho\phi\langle k\rangle^{\mathrm{i}}|\overline{\mathbf{u}}_{\mathrm{D}}/\sqrt{K}$ and

$$\begin{aligned}\rho&\left[\frac{\partial}{\partial t}\left(\phi\langle\varepsilon\rangle^{\mathrm{i}}\right) + \nabla\cdot\left(\overline{\mathbf{u}}_{\mathrm{D}}\langle\varepsilon\rangle^{\mathrm{i}}\right)\right]\\ &= \nabla\cdot\left[\left(\mu + \frac{\mu_{\mathrm{t}\phi}}{\sigma_\varepsilon}\right)\nabla\left(\phi\langle\varepsilon\rangle^{\mathrm{i}}\right)\right] + \frac{\langle\varepsilon\rangle^{\mathrm{i}}}{\langle k\rangle^{\mathrm{i}}}[c_1P^{\mathrm{i}} + c_2(G^{\mathrm{i}} - \rho\phi\langle\varepsilon\rangle^{\mathrm{i}})],\end{aligned} \tag{9}$$

where c_1, c_2, and c_k are constants, P^{i} is the production rate of $\langle k\rangle^{\mathrm{i}}$ due to gradients of $\overline{\mathbf{u}}_{\mathrm{D}}$, and G^{i} the generation rate of the intrinsic average of k due to the action of the porous matrix.

2.3 Interface and "Jump" Conditions

The equation proposed by Ochoa-Tapia and Whitaker (1995a,b) for describing the stress jump at the interface has been modified in Silva and de Lemos (2003b) to consider turbulent flow, in the form,

$$\begin{aligned}&\left(\mu_{\mathrm{eff}} + \mu_{\mathrm{t}\phi}\right)\frac{\partial\overline{u}_{\mathrm{Dp}}}{\partial y}\bigg|_{\text{Porous Medium}} - (\mu + \mu_{\mathrm{t}})\frac{\partial\overline{u}_{\mathrm{Dp}}}{\partial y}\bigg|_{\text{Clear Fluid}}\\ &\quad = (\mu + \mu_{\mathrm{t}})\frac{\beta}{\sqrt{K}}\,\overline{u}_{\mathrm{Dp}}\bigg|_{\text{interface}},\end{aligned} \tag{10}$$

where u_{Dp} is the Darcy velocity component parallel to the interface, μ_{eff} is the effective viscosity for the porous region, which according to Ochoa-Tapia and Whitaker (1995a,b) is given by $\mu_{\mathrm{eff}} = \mu/\phi$, and β an adjustable coefficient that accounts for the stress jump at the interface. Continuity of velocity, pressure, statistical variables, and their fluxes across the interface are given by (see Silva and de Lemos 2003b for details),

$$\overline{\mathbf{u}}_{\mathrm{D}}\big|_{\text{Porous Medium}} = \overline{\mathbf{u}}_{\mathrm{D}}\big|_{\text{Clear Fluid}} \tag{11}$$

$$\langle\overline{p}\rangle^{\mathrm{i}}\big|_{\text{Porous Medium}} = \langle\overline{p}\rangle^{\mathrm{i}}\big|_{\text{Clear Fluid}} \tag{12}$$

$$\langle k\rangle^{\mathrm{v}}\big|_{\text{Porous Medium}} = \langle k\rangle^{\mathrm{v}}\big|_{\text{Clear Fluid}} \tag{13}$$

$$\left(\mu+\frac{\mu_{\mathrm{t}\phi}}{\sigma_k}\right)\frac{\partial\langle k\rangle^{\mathrm{v}}}{\partial y}\bigg|_{\text{Porous Medium}} = \left(\mu+\frac{\mu_{\mathrm{t}}}{\sigma_k}\right)\frac{\partial\langle k\rangle^{\mathrm{v}}}{\partial y}\bigg|_{\text{Clear Fluid}} \tag{14}$$

$$\langle \varepsilon\rangle^{\mathrm{v}}\big|_{\text{Porous Medium}} = \langle \varepsilon\rangle^{\mathrm{v}}\big|_{\text{Clear Fluid}} \tag{15}$$

$$\left(\mu+\frac{\mu_{\mathrm{t}\phi}}{\sigma_\varepsilon}\right)\frac{\partial\langle \varepsilon\rangle^{\mathrm{v}}}{\partial y}\bigg|_{\text{Porous Medium}} = \left(\mu+\frac{\mu_{\mathrm{t}}}{\sigma_\varepsilon}\right)\frac{\partial\langle \varepsilon\rangle^{\mathrm{v}}}{\partial y}\bigg|_{\text{Clear Fluid}} \tag{16}$$

Equations 11 and 12 were also proposed by Ochoa-Tapia and Whitaker (1995a), whereas relationships (13) through (16) were used by Lee and Howell (1987).

In Silva and de Lemos (2003b), no "jump" condition was considered when treating the diffusion flux of $\langle k\rangle^{\mathrm{v}}$ across the interface, as can be seen by Eq. 14. In de Lemos (2005b), such discontinuity in the diffusion transport of $\langle k\rangle^{\mathrm{v}}$ and $\langle \varepsilon\rangle^{\mathrm{i}}$ between the two media was first proposed.

Before continuing, a word about the physical reasoning for proposing a discontinuity also for the turbulent field seems timely. Such "jump" might be a model for accounting for interface roughness or be a way to comply with irregular interfaces. In addition, it can also be seen as an accommodation of the fact that, close to the interface, the permeability K attains higher values than those used within the porous substrate. One can also mention that, for turbulent flow, momentum carries turbulence energy and if a discontinuity of time-mean momentum diffusion applies across the interface, then it is reasonable to infer that a discontinuity might also exist when transporting k across the same interface. In fact, decomposing properties in "mean" and "fluctuating" components is the sole outcome of application of statistical tools. The property itself has an instantaneous local value. If for the time-mean momentum equation a diffusion-jump applies, then for the same reason a diffusion-jump for k is also justifiable. For that, the interface condition of de Lemos (2005b) is here considered,

$$\left(\mu_{\mathrm{eff}}+\frac{\mu_{\mathrm{t}\phi}}{\sigma_k}\right)\frac{\partial\langle k\rangle^{\mathrm{v}}}{\partial y}\bigg|_{\text{Porous Medium}} - \left(\mu+\frac{\mu_{\mathrm{t}}}{\sigma_k}\right)\frac{\partial\langle k\rangle^{\mathrm{v}}}{\partial y}\bigg|_{\text{Clear Fluid}}$$
$$= \left(\mu+\frac{\mu_{\mathrm{t}}}{\sigma_k}\right)\frac{\beta_{\mathrm{t}}}{\sqrt{K}}\langle k\rangle^{\mathrm{v}}\bigg|_{\text{Interface}} \tag{17}$$

and for $\langle \varepsilon\rangle^{\mathrm{i}}$ it reads,

$$\left(\mu_{\mathrm{eff}}+\frac{\mu_{\mathrm{t}\phi}}{\sigma_\varepsilon}\right)\frac{\partial\langle \varepsilon\rangle^{\mathrm{v}}}{\partial y}\bigg|_{\text{Porous Medium}} - \left(\mu+\frac{\mu_{\mathrm{t}}}{\sigma_\varepsilon}\right)\frac{\partial\langle \varepsilon\rangle^{\mathrm{v}}}{\partial y}\bigg|_{\text{Clear Fluid}}$$
$$= \left(\mu+\frac{\mu_{\mathrm{t}}}{\sigma_\varepsilon}\right)\frac{\beta_{\mathrm{t}}}{\sqrt{K}}\langle \varepsilon\rangle^{\mathrm{v}}\bigg|_{\text{Interface}} \tag{18}$$

instead of Eqs. 14 and 16, respectively. Note that in de Lemos (2005b), the left-hand side of (17) assumed a value for σ_k equal to unity, which was the value used in his simulations. Also, to emphasize that a different jump coefficient might be needed for the turbulence equations, symbol β_{t} is used on the left of (17) and (18), instead of β. More on the use of a different jump coefficient for the turbulent flow equations will be discussed below. Conditions (17) and (18) are imposed along the interface shown in Fig. 1a.

Equations 17 and 18 result from the following reasoning, which is here discussed in some more details than in de Lemos (2005b). If interface condition (10) is written in its instantaneous form and recalling its proposition for flows parallel to the interface, it gives

$$\mu_{\mathrm{eff}} \frac{\partial \mathbf{u}_{\mathrm{Di}}}{\partial y}\bigg|_{\text{Porous Medium}} - \mu \frac{\partial \mathbf{u}_{\mathrm{Di}}}{\partial y}\bigg|_{\text{Clear Fluid}} = \mu \frac{\beta}{\sqrt{K}}\, \mathbf{u}_{\mathrm{Di}}\bigg|_{\text{interface}}. \tag{19}$$

After time-averaging (19) and considering the turbulent viscosity, one gets,

$$\begin{aligned}\left(\mu_{\mathrm{eff}} + \mu_{\mathrm{t}\phi}\right) \frac{\partial \overline{\mathbf{u}}_{\mathrm{Di}}}{\partial y}\bigg|_{\text{Porous Medium}} &- (\mu + \mu_{\mathrm{t}}) \frac{\partial \overline{\mathbf{u}}_{\mathrm{Di}}}{\partial y}\bigg|_{\text{Clear Fluid}} \\ &= (\mu + \mu_{\mathrm{t}}) \frac{\beta}{\sqrt{K}}\, \overline{\mathbf{u}}_{\mathrm{Di}}\bigg|_{\text{interface}}. \end{aligned} \tag{20}$$

Assuming now that the Darcy velocity at the interface varies with time, a standard time decomposition for it can be written as $\mathbf{u}_{\mathrm{Di}} = \overline{\mathbf{u}}_{\mathrm{Di}} + \mathbf{u}'_{\mathrm{Di}}$. Next, considering that only velocities fluctuate in time, subtracting (20) from (19) with turbulent viscosity results in the following relationship for the fluctuating interface velocity $\mathbf{u}'_{\mathrm{Di}}$,

$$\begin{aligned}\left(\mu_{\mathrm{eff}} + \mu_{\mathrm{t}\phi}\right) \frac{\partial \mathbf{u}'_{\mathrm{Di}}}{\partial y}\bigg|_{\text{Porous Medium}} &- (\mu + \mu_{\mathrm{t}}) \frac{\partial \mathbf{u}'_{\mathrm{Di}}}{\partial y}\bigg|_{\text{Clear Fluid}} \\ &= (\mu + \mu_{\mathrm{t}}) \frac{\beta}{\sqrt{K}}\, \mathbf{u}'_{\mathrm{Di}}\bigg|_{\text{interface}}. \end{aligned} \tag{21}$$

Taking the scalar product of $\mathbf{u}'_{\mathrm{Di}}$ and Eq. 21, one gets

$$\begin{aligned}(\mu_{\mathrm{eff}} + \mu_{\mathrm{t}\phi}) &\frac{\partial\left((\mathbf{u}'_{\mathrm{Di}} \cdot \mathbf{u}'_{\mathrm{Di}})/2\right)}{\partial y}\bigg|_{\text{Porous Medium}} \\ -(\mu + \mu_{\mathrm{t}}) &\frac{\partial\left((\mathbf{u}'_{\mathrm{Di}} \cdot \mathbf{u}'_{\mathrm{Di}})/2\right)}{\partial y}\bigg|_{\text{Clear Fluid}} \\ = (\mu + \mu_{\mathrm{t}}) &\frac{\beta}{\sqrt{K}} \left((\mathbf{u}'_{\mathrm{Di}} \cdot \mathbf{u}'_{\mathrm{Di}})/2\right)\bigg|_{\text{interface}}. \end{aligned} \tag{22}$$

If one now applies the time-averaging operation to Eq. 22 and note that the turbulence kinetic energy at the interface is given by $\langle k \rangle^{\mathrm{v}} = \overline{\mathbf{u}'_{\mathrm{Di}} \cdot \mathbf{u}'_{\mathrm{Di}}}/2$, condition (17) is recovered after introducing the constant σ_k and using β_{t}, instead of β. Similar arguments would have led to (18), which represents the rate at which $\langle k \rangle^{\mathrm{v}}$ is dissipated as it crosses the interface. Had a corresponding diffusion-jump model for $\langle \varepsilon \rangle^{\mathrm{v}}$ not been applied, then a possible unbalance among generation, transport, and dissipation of turbulent energy across the interface would occur. This situation would possibly lead to physical and numerical instabilities. This investigation, however, was not the objective of this study. Here, both macroscopic equations for k and ε considered a jump at the interface.

Further, as already observed in de Lemos (2005b), one should clarify that a different coefficient β_{t} might be necessary on the right-hand side of (17) and (18) to accommodate real engineering flows over porous substrates with rough interfaces, above vegetation, forest, crops, finite engineering equipment, or any other condition which might cause the use of β to be inadequate. Propositions (17) and (18), as such, should be regarded as a first step toward realistic modeling subjected to improvements as more experimental data on macroscopic interfaces become available.

Also, one should emphasize that the only continuum intrinsic variable across the interface is the liquid pressure because pressure on both sides of the liquid phase, at the interface, has to be the same. Other intrinsic quantities cannot be continuous if one side of the interface contains less void space. For example, for one-dimensional flows normal to the interface, the intrinsic fluid velocity $\langle \mathbf{u} \rangle^{\mathrm{i}}$ has to increase (be discontinuous) as the fluid enters the porous material. However, the same mass flow rate, and therefore $\mathbf{u}_{\mathrm{D}}$, flows from the clear region to the inside the porous matrix. By the same token, in Eqs. 14–18, the terms referent to the clear side will have the intrinsic average equal to the volumetric average ($\langle\rangle^{\mathrm{v}} = \langle\rangle^{\mathrm{i}}$) because, in the clear region, there is no solid material to differentiate between these two values. Likewise, in the clear region, the turbulent viscosity is given by μ_{t}. Further, it is important to note that Eq. 8 is valid for inside the porous medium where no jump is considered. Equation 17, on the other hand, compares the difference between the stresses on both sides of the interface. Equation 17 is not derived from Eq. 8, but it is a model to accommodate the assumption that shear stresses on both sides of the interface present a possible unbalance. If one has $\mu_{\mathrm{t}\phi} = \phi\mu_{\mathrm{t}}$ with $\mu_{\mathrm{t}} = \rho c_{\mu} \langle k \rangle^{\mathrm{v}^2} / \langle \varepsilon \rangle^{\mathrm{v}}$, $\mu_{\mathrm{eff}} = \mu/\phi$, $\langle k \rangle^{\mathrm{v}} = \phi \langle k \rangle^{\mathrm{i}}$, Eq. 17 is readily applicable as a suitable jump condition when Eq. 8 is used on the porous medium side ($\phi < 1$) and on the clear side ($\phi = 1$, $\langle k \rangle^{\mathrm{v}} = \langle k \rangle^{\mathrm{i}} = k$, $\mu_{\mathrm{t}\phi} = \mu_{\mathrm{t}}$) of the interface.

3 Numerical Details

Figure 1b shows a general control volume in a two-dimensional configuration (Patankar 1980). The faces of the volume are formed by lines of constant coordinates η–ξ. The work in Silva and de Lemos (2003a) was set up for solving one-dimensional laminar flows in the geometry of Fig. 1a and employed the spatially periodic boundary condition along the x coordinate. This was done to simulate fully developed flow. An imposed mass flow rate was set in the beginning of the calculations, which was maintained during the entire iterative process. Pressure distribution was calculated along with the relaxation of the algebraic equation system (Patankar 1980) and was not imposed anywhere in the channel. Pressure was the outcome of the numerical solution and for less permeable porous layers, a higher pressure head along the channel was necessary to maintain the imposed mass flow rate. The spatially periodic condition was implemented by running the 2D solution repetitively, until outlet profiles in $x = L$ matched those at the inlet ($x = 0$). Details on the methodology here employed for simulating fully developed flow using a two-dimensional numerical tool and the periodic condition along the x-direction can be found in Pedras and de Lemos (2001b,c, 2003).

In Silva and de Lemos (2003a), the discretization methodology used for including the jump condition in the numerical solutions was discussed. For that, only brief comments about the numerical procedure are made here. Also, details of the discretization of the terms on the left of (10) can be found in Pedras and de Lemos (2001b). Furthermore, information on the discretization of the right of (10) appears in Silva and de Lemos (2003a) where more particulars can be found. Here, attention is focused on the numerical treatment of (17) and (18), whose discretization followed the nomenclature shown in Fig. 1b.

For steady state, a general form of the discrete equations for a general variable φ becomes

$$I_e + I_w + I_n + I_s = S_\varphi, \tag{23}$$

where I_{e}, I_{w}, I_{n}, and I_{s} are the fluxes of φ at faces *east*, *west*, *north*, and *south* of the control volume of Fig. 1b, respectively, and S_φ is a source term. Here, all computations were carried out until normalized residues of the algebraic equations were brought down to 10^{-7}.

Figure 1c shows details of the interface dividing two control volumes, one being located in the porous region and the other lying in the clear fluid. The computational grid based on generalized coordinate system η–ξ is such that the interface coincides with a line of constant

η, extending itself along the ξ coordinate. In this arrangement, the interface between the two neighbor volumes, each one located on each side of the interface, belongs to both faces of the two volumes. Thus, according to the Fig. 1c, $\bar{\mathbf{u}}_{\mathrm{Di}}$ is the Darcy velocity at the interface and $\bar{\mathbf{u}}_{\mathrm{Dp}}$ its component parallel to the interface.

Also, one should emphasize that for the sake of simplicity in notation, a volume-average velocity is given the symbol $\bar{\mathbf{u}}_{\mathrm{D}} = \phi\langle\bar{\mathbf{u}}\rangle^{\mathrm{i}}$. If the computational node is outside the porous substrate, one gets $\bar{\mathbf{u}}_{\mathrm{D}} = \langle\bar{\mathbf{u}}\rangle^{\mathrm{i}}$ since, by definition, porosity is equal to unity in the free flow region. Accordingly, due to the numerical methodology used in this work (control-volume), no distinction is made if a variable is averaged in a control-volume having only "liquid" (free flow or clear domain) or in a control-volume containing a "solid" phase (porous matrix). Therefore, one always is referring to a volume-based numerical value, either in the fluid or in the porous medium.

Further, in Fig. 1c one can identify all variables located at the interface. The modulus of the macroscopic interfacial area can be expressed as

$$|\mathbf{A}_{\mathrm{i}}| = A_{\mathrm{i}} = \ell_{\mathrm{i}} \times 1 = \sqrt{(x_{\mathrm{ne}} - x_{\mathrm{nw}})^2 + (y_{\mathrm{ne}} - y_{\mathrm{nw}})^2}. \tag{24}$$

Integrating the left-hand side of (17) over the macroscopic interfacial area A_{i}, and considering further constant $\langle k\rangle^{\mathrm{i}}$ and constant properties prevailing over the integration area, one has

$$I_{\mathrm{i}}^{\beta_k} = \int_{A_{\mathrm{i}}} \left(\mu + \frac{\mu_{\mathrm{t}}}{\sigma_k}\right) \frac{\beta_{\mathrm{t}}}{\sqrt{K}} \langle k\rangle^{\mathrm{v}}\Big|_{\mathrm{i}} \mathrm{d}A_{\mathrm{i}} \approx \left(\mu + \frac{\mu_{\mathrm{t}}}{\sigma_k}\right)_{\mathrm{i}} \frac{\beta_{\mathrm{t}}}{\sqrt{K}} \langle k\rangle^{\mathrm{v}}\Big|_{\mathrm{i}} A_{\mathrm{i}} \tag{25}$$

or

$$\begin{aligned} I_{\mathrm{i}}^{\beta_k} &\approx \left(\mu + \frac{\mu_{\mathrm{t}}}{\sigma_k}\right)_{\mathrm{i}} \frac{\beta_{\mathrm{t}}}{\sqrt{K}} \langle k\rangle^{\mathrm{v}}\Big|_{\mathrm{i}} A_{\mathrm{i}} = \left(\mu + \frac{\mu_{\mathrm{t}}}{\sigma_k}\right)_{\mathrm{i}} \frac{\beta_{\mathrm{t}}}{\sqrt{K}} \langle k\rangle^{\mathrm{v}} \ell_{\mathrm{i}} \\ &= \left(\mu + \frac{\mu_{\mathrm{t}}}{\sigma_k}\right)_{\mathrm{i}} \frac{\beta_{\mathrm{t}}}{\sqrt{K}} \langle k\rangle^{\mathrm{v}} \sqrt{(x_{\mathrm{ne}} - x_{\mathrm{nw}})^2 + (y_{\mathrm{ne}} - y_{\mathrm{nw}})^2}. \end{aligned} \tag{26}$$

Following similar steps for the ε-equation, one gets

$$\begin{aligned} I_{\mathrm{i}}^{\beta_\varepsilon} &\approx \left(\mu + \frac{\mu_{\mathrm{t}}}{\sigma_\varepsilon}\right)_{\mathrm{i}} \frac{\beta_{\mathrm{t}}}{\sqrt{K}} \langle \varepsilon\rangle^{\mathrm{v}}\Big|_{\mathrm{i}} A_{\mathrm{i}} = \left(\mu + \frac{\mu_{\mathrm{t}}}{\sigma_\varepsilon}\right)_{\mathrm{i}} \frac{\beta_k}{\sqrt{K}} \langle \varepsilon\rangle^{\mathrm{v}} \ell_{\mathrm{i}} \\ &= \left(\mu + \frac{\mu_{\mathrm{t}}}{\sigma_\varepsilon}\right)_{\mathrm{i}} \frac{\beta_{\mathrm{t}}}{\sqrt{K}} \langle \varepsilon\rangle^{\mathrm{v}} \sqrt{(x_{\mathrm{ne}} - x_{\mathrm{nw}})^2 + (y_{\mathrm{ne}} - y_{\mathrm{nw}})^2}. \end{aligned} \tag{27}$$

The terms on the right of (26) and (27) are added to the discretized k- and ε-equation components, respectively, when the nodal point in question has a face coincident with the interface. For ease of implementation, these additional terms are treated in an explicit form and are added to the right-hand side of (23).

Before proceeding, it is important to emphasize the following. It is a well-known feature in the turbulence modeling community that when using standard k–ε models, profiles of ε follows the same features as those of the results of k. The reason is that such standard two-equation model is based on two quantities that are intimately linked by one unique time scale, which measures k/ε. Therefore, major features in the k behavior are as well reflected in its dissipation rate. For example, in boundary layer flows close to walls, the rise of levels of k is accompanying by an elevation on ε values, otherwise no balance between production of turbulent kinetic energy and its dissipation rate would result in a physically stable solution. For this reason, rarely in the literature, results for ε are also presented in conjunction with simulations for k, which is, in fact, the important quantity for which simulations are performed. Distinct two-equation models such as k–ℓ, k–ω, and others, also aim at simulating the behavior or k being the secondary transported quantity of a less important nature. Essentially, a velocity scale ($k^{1/2}$), and a length scale ($\ell = k^{3/2}/\varepsilon$ in the particular case of k–ε model) are needed to characterize the turbulent eddy viscosity. Accordingly, in this work, attention is focused on the numerical results obtained for k.

4 Results and Discussion

The flow in Fig. 1a was computed with the set of Eqs. 4, 8, and 9 with additional constitutive Eq. 5 and the macroscopic Kolmogorov–Prandtl expression (7). The wall function approach was used for treating the flow close to the wall. Grid independence studies were conducted in Silva and de Lemos (2003a) and, for more than 40 nodal points in the cross-stream direction, the solution was essentially grid independent. One should emphasize that the numerical methodology here considered was focused on two-dimensional flows, so that simulating the fully developed situation shown in the figure required the use of nodal points along the axial direction as well as the employment of the spatially periodic condition mentioned earlier. For all runs studied here, a total of 50 nodes in the axial direction were found to suffice. It is also important to note that the sign of coefficient β in expression (10) and (17) depends on the orientation of the y-axis in relation to the porous layer location. Here, the same orientation given by Kuznetsov (1996, 1997, 1999) was used, which considers the porous layer at the top of the channel with its normal pointing toward the minus y-direction. In this article, simulations with positive and negative values of β were conducted to investigate its effect on the profiles of mean velocity and k. Determination of its numerical values, however, was not the objective of this work. One possibility to obtain β is to resolve numerically for the intra-pore flow structure with a fine computational grid, volume-average the results, and compare the macroscopic values with models such as the diffusion-jump model.

As such, coherent computations for laminar flow (Silva and de Lemos 2003a) were obtained. As mentioned, grid independence studies were carried out by Silva and de Lemos (2003a), indicating the proper number of nodal points used around the interface. There, the authors correctly reproduced, with their numerical tool, the boundary layers around the interface proposed by the analytical study of Kuznetsov (1996, 1997, 1999). Also, for the case of turbulent flow, the number of grid point used seems to be appropriate. In all computations herein, the following condition and values were used (de Lemos 2005b, Lee and Howell 1987): $\beta_t = \beta$, $c_\mu = 0.09$, $c_1 = 1.44$, $c_2 = 1.92$, $c_k = 0.28$, $\sigma_k = 1.0$ and $\sigma_\varepsilon = 1.33$. It is also important to mention that while comparisons with experimental results greatly benefits and are paramount to evaluation of any theoretical and numerical analyses, the set of results herein focus on the behavior of the model as certain parameters are varied. Full model evaluation and verification is under way, and shall be the subject of future work.

The effect of $\mathrm{Re_H}$ is shown in Fig. 2. Plots on the left (a, c) are for mean velocity, whereas curves on the right of the figure (b, d) details the behavior of the turbulent filed. Also, drawings on the top (a, b) were calculated for $\beta < 0$, whereas figures on the bottom (c, d) used positive values of β. The mean velocity profiles in Fig. 2a and c confirms the increasing mass flow rate within either the porous material or the clear passage as $\mathrm{Re_H}$ increases. In Fig. 2b and d, the collapse of curves for the turbulent kinetic energy divided by the mean mechanical energy shows that, for the range of $\mathrm{Re_H}$ analyzed here, the percentage of energy transformed into turbulence remains the same, regardless of the diffusion-jump model used. The most striking feature in Fig. 2 is the different response, in the turbulence field (b, d), when using values for β of different sign. Negative values for β (Fig. 2b) indicate that the peaks in the curves lie lower than when no jump condition is used, and that this peak is at the interface.

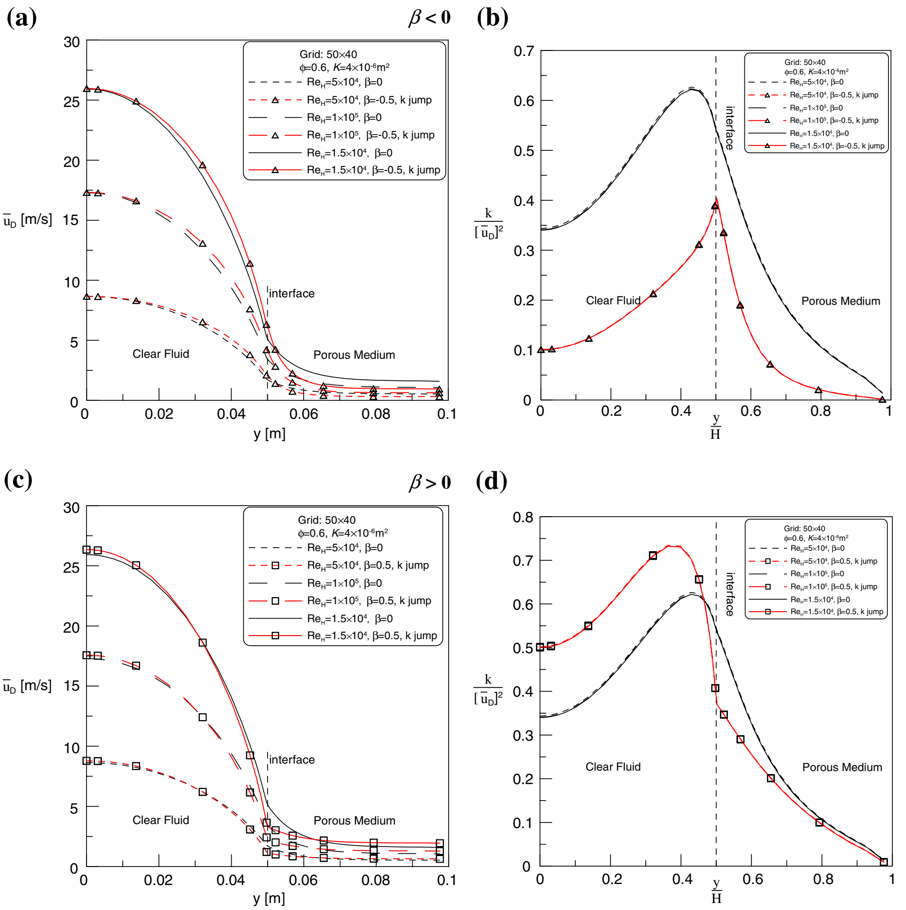

Fig. 2 Effect of Reynolds number, $\mathrm{Re_H}$, on macroscopic field. $\beta \leq 0$: **a** mean velocity, **b** turbulent kinetic energy; $\beta \geq 0$: **c** mean velocity, **d** turbulent kinetic energy

On the other hand, for a positive β, the levels of k are higher than if no jump condition is applied. In addition, the peaks are moved toward the center of the channel. The behavior of the curves is associated with corresponding mean velocity profiles. Within the clear fluid, the production of turbulent kinetic energy is known to be dictated by gradients of the mean velocity (P^{i} on the right of (8)), whereas inside the permeable structure, the model of Pedras and de Lemos (2001a) proposes a factor proportional to $\bar{\mathbf{u}}_{\mathrm{D}}$ as a generating mechanism for $k(G^{\mathrm{i}}$ in Eq. 8).

Figure 3 shows the effect of the permeability K on both the mean and statistical fields. Plots a, b, c, and d follow the same convention described in Fig. 2. The figure indicates that, the greater the permeability, more flow crosses the porous substratum located in the region $0.5 < y/H < 1$ (Fig. 3a–c). The curves representing the statistical field in Fig. 3b–d show that the levels of k increase with increasing K. As more fluid flows in less resistant media, more mean mechanical energy is transformed into turbulence increasing the overall level of k.

Finally, Fig. 4 investigates the effect of the value of ϕ on the behavior of the mean and turbulent fields, here also following the same convention established when presenting Fig. 2 (plots a, b, c, and d). For the mean field (a, c), one can note that close to y/H=0.5 the

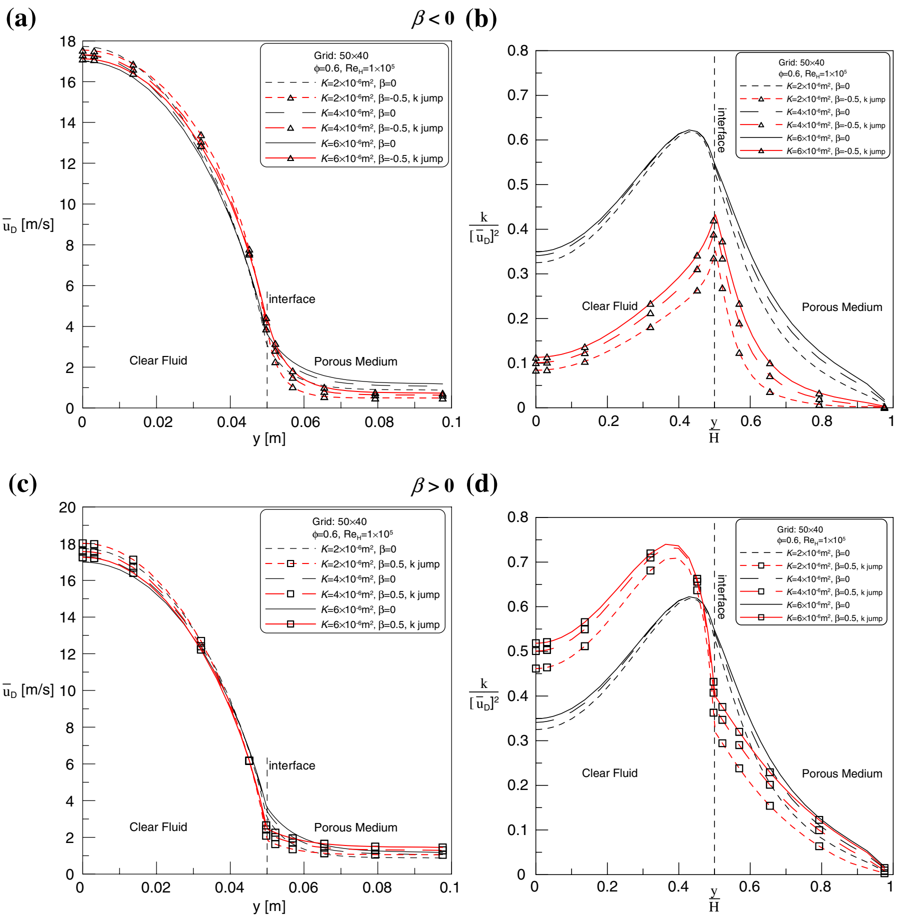

Fig. 3 Effect of permeability, K, on macroscopic field. $\beta \leq 0$: **a** mean velocity, **b** turbulent kinetic energy; $\beta \geq 0$: **c** mean velocity, **d** turbulent kinetic energy

greater the porosity, the higher the velocity at the interface, and the greater the mass flow rate closer to this region. At the center of the channel, the velocity decreases to keep the imposed mass flow rate the same. It is interesting to observe that since the overall mass flow rate is forced to be constant, instead of the overall pressure loss along the channel, an enhancement of the mass flow rate along the porous bed in the interface region is compensated by a slight reduction on local velocities close to the wall. Figure 4b–d shows corresponding curves for the behavior of the turbulent kinetic energy. Values of k present a slight reduction as ϕ is incremented. Lower values for the turbulence level within the porous layer are coherent with the model of Eq. 8 for the extra generation rate due to the porous matrix. As said, this extra G^{i} term (3rd on the right of (8)) was modeled as proportional to $\bar{\mathbf{u}}_{\mathrm{D}}$ and, inside the porous layer, the mean Darcy velocity is reduced as ϕ increases.

Ultimately, results in Figs. 2, 3, and 4 indicates that for flows where models with $\beta < 0$ are suitable, a smaller portion of the mean mechanical energy of the flow is converted into turbulence. Results herein might be useful to environmentalists and engineers analyzing important natural and engineering flows. Although in the porous substrate, mean velocity profiles are flatter, reducing the production rate P^{i}, the generating mechanism G^{i} is proportional to $\bar{\mathbf{u}}_{\mathrm{D}}$,

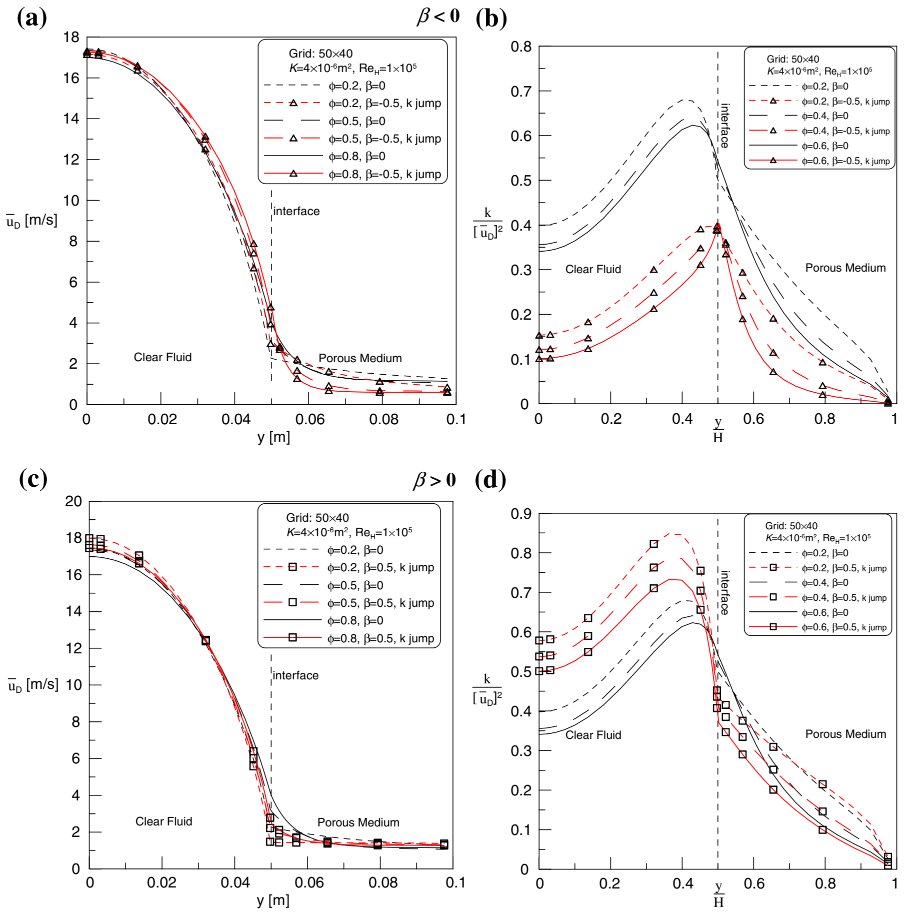

Fig. 4 Effect of porosity, ϕ, on macroscopic field. $\beta \leq 0$: **a** mean velocity, **b** turbulent kinetic energy; $\beta \geq 0$: **c** mean velocity, **d** turbulent kinetic energy

increases the overall value of k. In the clear fluid, steeper gradients in the fluid layer also contributes for increasing the value of the turbulent kinetic energy. Then, either by P^{i} in the clear fluid or by G^{i} in the porous layer, turbulent kinetic energy is generated at a faster rate for positive values of β.

5 Concluding Remarks

For flat interfaces, numerical solutions for turbulent flow in composite channels were obtained for different values of $\mathrm{Re_H}$, K, and β parameters. Results were compared with previous computations by Silva and de Lemos (2003b), which did not include a diffusion jump for k. Inclusion of such term resulted in qualitatively different profiles for the turbulence kinetic energy, ultimately indicating a different portion of the available mechanical energy that is converted into turbulence. Although simulations were presented for one-dimensional flows, the implementation herein was done for two-dimensional situations and carried out on a generalized coordinate system.

Results herein may contribute to the analysis of important environmental and engineering flows, where an irregular interface surrounding a porous body may be identified. Future applications of the model may be useful in determining the overall exchange rates of energy and mass transport across a interface between a porous medium and a clear region.

Acknowledgements The author is thankful to CNPq, CAPES and FAPESP, Brazil, for their invaluable financial support during the course of this research.

References

Assato, M., Pedras, M.H.J., de Lemos, M.J.S.: Numerical solution of turbulent channel flow past a backward-facing step with a porous insert using linear and nonlinear k–ε models. J. Porous Media **8**(1), 13–29 (2005) doi:10.1615/JPorMedia.v8.i1.20

Braga, E.J., de Lemos, M.J.S.: Turbulent natural convection in a porous square cavity computed with a macroscopic k-ε model. Int. J. Heat Mass Transf. **47**(26), 5639–5650 (2004) doi:10.1016/j.ijheatmasstransfer.2004.07.017

Breugem, W.P., Boersma, B.J.: Direct numerical simulations of turbulent flow over a permeable wall using a direct and a continuum approach. Phys. Fluids **17**(2), (2005) doi:10.1063/1.1835771

de Lemos, M.J.S.: Fundamentals of the double—decomposition concept for turbulent transport in permeable media. Materialwiss. Werkstofftech. **36**(10), 586–593 (2005a) doi:10.1002/mawe.200500910

de Lemos, M.J.S.: Turbulent kinetic energy distribution across the interface between a porous medium and a clear region. Int. Comm. Heat Mass Transf. **32**(1–2), 107–115 (2005b) doi:10.1016/j.icheatmasstransfer.2004.06.011

de Lemos, M.J.S.: Turbulence in Porous Media: Modeling and Applications. Elsevier, Kindlington (2006)

de Lemos, M.J.S.: Analysis of turbulent flows in fixed and moving permeable media. Acta Geophys. **56**(3), 562–583 (2008) doi:10.2478/s11600-008-0026-x

de Lemos, M.J.S., Braga, E.J.: Modeling of turbulent natural convection in saturated rigid porous media. Int. Comm. Heat Mass Transf. **30**(5), 615–624 (2003) doi:10.1016/S0735-1933(03)00099-X

de Lemos, M.J.S., Mesquita, M.S.: Turbulent mass transport in saturated rigid porous media. Int. Comm. Heat Mass Transf. **30**(1), 105–113 (2003) doi:10.1016/S0735-1933(03)00012-5

de Lemos, M.J.S., Pedras, M.H.J.: Simulation of turbulent flow through hybrid porous medium-clear fluid domains. In: Proceedings of IMECE2000 - ASME - International Mechanical Engineering Congress, ASME-HTD-366-5, ISBN 0-7918-1908-6, pp. 113–122. Orlando, Florida (2000)

de Lemos, M.J.S., Pedras, M.H.J.: Recent mathematical models for turbulent flow in saturated rigid porous media. ASME. J. Fluids Eng. **123**(4), 935–940 (2001) doi:10.1115/1.1413243

de Lemos, M.J.S., Silva, R.A.: Turbulent flow around a wavy interface between a porous medium and a clear domain. In: Proceedings of ASME-FEDSM2003- Fluids Engineering Division Summer Meeting, Paper FEDSM2003-45457 (on CD-ROM), Honolulu, Hawaii, USA, 6–11 July 2003

de Lemos, M.J.S., Tofaneli, L.A.: Modeling of double-diffusive turbulent natural convection in porous media. Int. J. Heat Mass Transf. **47**(19–20), 4221–4231 (2004)

Finnigan, J.: Turbulence in plant canopies. Annu. Rev. Fluid Mech. **32**, 519–571 (2000) doi:10.1146/annurev.fluid.32.1.519

Gray, W.G., Lee, P.C.Y.: On the theorems for local volume averaging of multiphase system. Int. J. Multiph. Flow **3**, 333–340 (1977) doi:10.1016/0301-9322(77)90013-1

Hoffmann, M.R.: Application of a simple space-time averaged porous media model to flow in densely vegetated channels. J. Porous Media **7**(3), 183–191 (2004) doi:10.1615/JPorMedia.v7.i3.30

Kuznetsov, A.V.: Analytical investigation of the fluid flow in the interface region between a porous medium and a clear fluid in channels partially filled with a porous medium. Int. J. Heat Fluid Flow **12**, 269–272 (1996)

Kuznetsov, A.V.: Influence of the stresses jump condition at the porous-medium/clear-fluid interface on a flow at a porous wall. Int. Comm. Heat Mass Transf. **24**, 401–410 (1997) doi:10.1016/S0735-1933(97)00025-0

Kuznetsov, A.V.: Fluid mechanics and heat transfer in the interface region between a porous medium and a fluid layer: a boundary layer solution. J. Porous Media **2**(3), 309–321 (1999)

Kuznetsov, A.V.: Numerical modeling of turbulent flow in a composite porous/fluid duct utilizing a two-layer k–ε model to account for interface roughness. Int. J. Therm. Sci. **43**(11), 1047–1056 (2004) doi:10.1016/j.ijthermalsci.2004.02.011

Lane, S.N., Hardy, R.J.: Porous rivers: a new way of conceptualizing and modeling river and floodplain flows? In: Ingham D., Pop I. (eds.) Transport Phenomena in Porous Media II, Chapt. 16 , 1st edn., pp. 425–449, Pergamon Press, NY (2002)

Launder, B.E., Spalding, D.B.: The numerical computation of turbulent flows. Comput. Methods Appl. Mech. Eng. **3**, 269–289 (1974) doi:10.1016/0045-7825(74)90029-2

Lee, K., Howell, J.R.: Forced convective and radiative transfer within a highly porous layer exposed to a turbulent external flow field. In: Proceedings of the 1987 ASME-JSME Thermal Engineering Joint Conference, vol. 2, pp. 377–386 (1987)

Nepf, H., Ghisalberti, M.: Flow and transport in channels with submerged vegetation. Acta Geophys. **56**(3), 753–777 (2008) doi:10.2478/s11600-008-0017-y

Ochoa-Tapia, J.A., Whitaker, S.: Momentum transfer at the boundary between a porous medium and a homogeneous fluid—I. Theoretical development. Int. J. Heat Mass Transf. **38**, 2635–2646 (1995a) doi:10.1016/0017-9310(94)00346-W

Ochoa-Tapia, J.A., Whitaker, S.: Momentum transfer at the boundary between a porous medium and a homogeneous fluid—II. Comparison with experiment. Int. J. Heat Mass Transf. **38**, 2647–2655 (1995b) doi:10.1016/0017-9310(94)00347-X

Patankar, S.V.: Numerical Heat Transfer and Fluid Flow. Hemisphere, New York (1980)

Pedras, M.H.J., de Lemos, M.J.S.: On the definition of turbulent kinetic energy for flow in porous media. Int. Comm. Heat Mass Trans. **27**(2), 211–220 (2000)

Pedras, M.H.J., de Lemos, M.J.S.: Macroscopic turbulence modeling for incompressible flow through undeformable porous media. Int. J. Heat Mass Transf. **44**(6), 1081–1093 (2001a) doi:10.1016/S0017-9310(00)00202-7

Pedras, M.H.J., de Lemos, M.J.S.: Simulation of turbulent flow in porous media using a spatially periodic array and a low re two-equation closure. Numer. Heat Transf. Part A Appl. **39**(1), 35–59 (2001b)

Pedras, M.H.J., de Lemos, M.J.S.: On mathematical description and simulation of turbulent flow in a porous medium formed by an array of elliptic rods. ASME. J. Fluids Eng. **123**(4), 941–947 (2001c) doi:10.1115/1.1413244

Pedras, M.H.J., de Lemos, M.J.S.: Computation Of turbulent flow in porous media using a low reynolds k–ε model and an infinite array of transversally-displaced elliptic rods. Numer. Heat Transf. Part A Appl. **43**(6), 585–602 (2003)

Poggi, D., Katul, G.G.: An experimental investigation of the mean momentum budget inside dense canopies on narrow gentle hilly terrain. Agric. For. Meteorol. **144**, 1–13 (2007) doi:10.1016/j.agrformet.2007.01.009

Prinos, P., Sofialidis, D., Keramaris, E.: Turbulent flow over and within a porous bed. J. Hydraul. Eng. **129**(9), 720–733 (2003) doi:10.1061/(ASCE)0733-9429(2003)129:9(720)

Prithiviraj, M., Andrews, M.J.: Three-dimensional numerical simulation of shell-and-tube heat exchanger part I—foundation and fluid mechanics. Numer. Heat Transf. Part A—Appl. **33**, 799–816 (1998)

Raupach, M.R., Shaw, R.H.: Averaging procedures for flow within vegetation canopies. Boundary-Layer Meteorol. **22**, 79–90 (1982) doi:10.1007/BF00128057

Rocamora, F.D., Jr., de Lemos, M.J.S.: Analysis of convective heat transfer for turbulent flow in saturated porous media. Int. Comm. Heat Mass Transf. **27**(6), 825–834 (2000a) doi:10.1016/S0735-1933(00)00163-9

Rocamora, F.D., Jr., de Lemos, M.J.S.: Laminar recirculating flow and heat transfer in hybrid porous medium-clear fluid computational domains. In: Proceedings of 34th ASME-National Heat Transfer Conference (on CD-ROM), ASME-HTD-I463CD, Paper NHTC2000-12317, ISBN 0-7918-1997-3, Pittsburgh, PA (2000b)

Sha, W.T.: A new porous-media approach for thermal-hydraulic analysis. Trans. ANS **39**, 510–512 (1981)

Silva, R.A., de Lemos, M.J.S.: Numerical analysis of the stress jump interface condition for laminar flow over a porous layer. Numer. Heat Transf. Part A Appl. **43**(6), 603–617 (2003a)

Silva, R.A., de Lemos, M.J.S.: Turbulent flow in a channel occupied by a porous layer considering the stress jump at the interface. Int. J. Heat Mass Transf. **46**(26), 5113–5121 (2003b) doi:10.1016/S0017-9310(03)00368-5

Silva, R.A., de Lemos, M.J.S.: Laminar flow around a sinusoidal interface between a porous medium and a clear fluid. In: Proceedings of COBEM2003 - 17th International Congress of Mechanical Engineering, Paper 1528 (on CD-ROM), São Paulo, Brazil, 10–14 Nov 2003

Whitaker, S.: Advances in theory of fluid motion in porous media. Ind. Eng. Chem. **61**, 14–28 (1969) doi:10.1021/ie50720a004

White, B., Nepf, H.M.: Scalar transport in random cylinder arrays at moderate Reynolds number. J. Fluid Mech. **487**, 43–79 (2003) doi:10.1017/S0022112003004579

Zhou, X.Y., Pereira, J.C.F.: A multidimensional model for simulating vegetation fire spread using a porous media sub-model. Fire Mater. **24**, 37–43 (2000) doi:10.1002/(SICI)1099-1018(200001/02)24:1<37::AID-FAM718>3.0.CO;2-Q